Toxicity-specific peripheral blood T and B cell dynamics in anti-PD-1 and combined immune checkpoint inhibition

Mick J.M. van Eijs,[1,2,#] Rik J. Verheijden,[1] Stefanie A. van der Wees,[2] Stefan Nierkens,[2,3] Anne S.R. van Lindert,[4] Karijn P.M. Suijkerbuijk[1,*], Femke van Wijk,[2,*] on behalf of the UNICIT Consortium

[1] Department of medical oncology, University Medical Center Utrecht, Utrecht, the Netherlands

[2] Center for Translational Immunology, University Medical Center Utrecht, Utrecht, the Netherlands

[3] Princess Máxima Center for Pediatric Oncology, Utrecht, the Netherlands

[4] Department of pulmonology, University Medical Center Utrecht, Utrecht, the Netherlands

*Contributed equally

[#] Corresponding author: Mick. J.M. van Eijs; Internal mail no. KC.02.085.2, P.O. Box 85090, 3508 AB, Utrecht, the Netherlands; m.j.m.vaneijs-2@umcutrecht.nl.

Collaborators UNICIT consortium: Linde Meyaard, Jürgen H.E. Kuball, Bas Oldenburg, Jeanette H.W. Leusen.

Abstract

Background Immune checkpoint inhibitors (ICI) have revolutionized the treatment landscape of advanced malignancies, but come with a diverse spectrum of immune-related adverse events (irAEs). Studies into irAE mechanisms are needed to make a transition from expert-opinion to evidence-based irAE treatment strategies.

Methods We aimed to longitudinally characterize peripheral blood T and B cell dynamics in ICI-treated patients developing irAEs and remaining irAE-free. PBMCs were immunophenotyped and functionally assessed with multicolor flow cytometry at baseline, after ±3 weeks and ±6 weeks or upon clinically relevant irAEs. Additionally, serum cytokine concentrations for 23 analytes were measured by multiplex immunoassay at the same timepoints.

Results We analyzed samples from 44 ICI-treated patients (24 anti-PD-1 monotherapy, 20 combined anti-PD-1 and anti-CTLA-4; cICI), of whom 22 developed clinically relevant irAEs, and 10 healthy donors. IrAEs after cICI were characterized by significantly enhanced proliferation of Th1-associated, mainly effector memory T cells, as well as Th17-associated and possibly antibody-mediated immune responses. The latter response was reflected in cICI toxicity by rising CXCL13 and IL-21 levels, but without changes in $CD21^{lo}$, memory, class-switched or newly activated B cell subsets. Anti-PD-1 monotherapy-inflicted irAEs were associated with a modestly enhanced Th1-associated response compared to irAE-free patients, only reflected by increasing serum CXCL9 and CXCL10, but without cellular changes in Th1/Tc1 subsets. $PD\text{-}1^{+}LAG\text{-}3^{+}$ double-positive (DP) $CD8^{+}$ T cells retained their proinflammatory potential in all treatment groups, regardless of irAE development. Especially DP $CD8^{+}$ T cells showed enhanced cytotoxic capacity in patients with irAEs after cICI. In all patients with irAEs, highly cytotoxic $CD57^{+}$ $CD8^{+}$ T cells were abundant.

Conclusions Peripheral blood immune responses are substantially different between cICI and anti-PD-1 monotherapy-treated patients. ICI-induced toxicity is clearly dominated by an enhanced Th1-associated response, but in cICI we also found evidence for Th17-associated and possibly antibody-mediated responses. $CD4^{+}$ effector memory T cells were the principal cycling cells in irAEs after cICI. Together, our data add to the growing body of evidence that irAEs may be antibody-mediated and driven by newly activated $CD4^{+}$ helper T cells, specifically after cICI.

Background

Immune checkpoint inhibitors (ICI) have realized unprecedented survival improvements in a selection of patients with advanced malignancies, but comes with a broad spectrum of immune-related adverse events (irAEs) [1]. To date, recommendations for irAE management are largely based on multidisciplinary expert consensus [2-4]. In quest of rationally developed treatment strategies, it has been suggested to draw on experience with specific autoimmune diseases (AD) these irAEs mimic, assuming shared pathophysiology [1]. Despite similarities, immune-related toxicity should clinically be considered a separate disease entity. This is, for instance, illustrated by the more acute onset, the possibility of complete irAE reversibility with adequate therapy and shorter time-to-response of biologicals [5]. Together with the concern that targeted immunosuppression may thwart antitumor immunity [6, 7], these observations underscore that evidence-based irAE treatment requires more profound biological understanding of specific mechanisms underlying ICI-induced toxicity.

Many efforts have been undertaken to predict irAEs at baseline or early on-treatment based on peripheral blood immune cells, cytokines, auto-antibodies and gut microbiome, as extensively reviewed in Hommes et al. [8]. Relatively higher blood lymphocyte count at baseline has been associated with development of irAEs [8]. Several studies that further characterized T and B cells at baseline and on-treatment reported a multitude of factors associated with irAE development, such as lower regulatory T cell function, baseline Th17 dominance and early increase in $CD21^{lo}$ B cells [9-13]. However, most of these findings still warrant replication and they do not reflect a mechanism common to all irAEs [13]. Particularly effector memory $CD4^+$ T cells ($CD4_{EM}$) have recently been suggested as drivers of irAEs [11, 14, 15]. $CD4^+$ T cell clonal expansion preceding irAEs [11, 16] and indications for epitope sharing between tumor and irAE-affected tissue [17, 18] suggests a role for T cell auto-reactivity in irAE development [11, 14]. However, the concept of genuine autoimmunity does not seem to completely recapitulate the pathophysiology of irAEs.

Although pathophysiological understanding has drastically improved over recent years, longitudinal studies into general irAE mechanisms comparing different ICI regimens are lacking, but urgently needed to improve irAE treatment strategies [19]. Besides, the role of B cells in irAEs has received little attention. Therefore, we interrogated peripheral T and B cell dynamics and cytokine production from baseline to several weeks on-treatment and upon immune-related toxicity in anti-PD-1 monotherapy and combined anti-CTLA-4 and anti-PD-1 (cICI) treated patients.

Methods

Study population and design

We included patients from the UNICIT biobank study conducted within the University Medical Center Utrecht, Utrecht, the Netherlands. Adult patients undergoing a first regimen of ICI with anti-PD-1 monotherapy, combined anti-CTLA-4 and anti-PD-1 (cICI), or anti-PD-(L)1 in combination with chemotherapy for a solid malignancy are

101 prospectively enrolled in this biobank, with >450 patients currently included and recruitment ongoing. Stool and
102 blood samples are collected at baseline, 3-4 weeks and 6-8 weeks after treatment initiation, and upon onset of
103 irAEs prior to initiation of immunosuppressive therapy. Furthermore, stool and blood samples are collected after
104 every new line immunosuppression administered for irAEs. If patients undergo diagnostic procedures for suspected
105 immune-mediated toxicity, extra biopsies of irAE affected tissue are obtained. Tumor response to ICI per RECIST
106 1.1 [ref. 20], irAE incidence and severity per CTCAE version 5 [ref. 21], as well as doses and duration of all
107 immunosuppressives administered for irAEs are continuously recorded.
108 Samples from patients treated with cICI or anti-PD-1 monotherapy (without chemotherapy) were used in
109 the present study. We included peripheral blood mononuclear cell (PBMC) and serum samples collected at
110 baseline, at 3-4 weeks for patients who were irAE-free at that time, and at 6-8 weeks for patients without clinically
111 relevant irAEs (NOTx) or at onset of irAEs for patients with clinically relevant toxicity (TOX). 'Clinically relevant
112 toxicity' was defined as CTCAE v5 grade ≥2 irAEs leading to 1) temporary or permanent ICI discontinuation, and
113 2) demanding hospitalization and/or ≥0.5 mg/kg daily prednisone as first-line immunosuppression. Blood samples
114 for healthy donor PBMCs were obtained from the University Medical Center Utrecht Mini Donor Service.
115
116 **Blood sample processing**
117 Blood was collected in clot-activating or sodium heparinized vacutainers (VACUETTE®, Greiner Bio-One, Austria).
118 Serum was isolated and frozen at -80°C within 4 hours after blood collection. PBMCs were isolated using Ficoll-
119 Paque (GE Healthcare, Chicago, IL) based density-gradient centrifugation, frozen in Roswell Park Memorial
120 Institute (RPMI) 1640 medium (Gibco, Grand Island, NY) supplemented with 2 mM L-glutamine (L-glu; Gibco), 100
121 IU/ml penicillin-streptomycin (p/s; Gibco), 20% fetal bovine serum (FBS; Invitrogen, Carlsbad, CA) and 10%
122 dimethyl sulfoxide (DMSO; Sigma-Aldrich, St. Louis, MO) and stored in the liquid phase of nitrogen until further use.
123
124 **Flow cytometry**
125 PBMCs were thawed in a 37°C water bath, washed twice and resuspended in RPMI 1640 medium supplemented
126 with 2 mM L-glu, 100 IU/ml p/s and 10% FBS and plated in round bottom 96-wells plates at a concentration of 0.5–
127 1.0×10^6 cells per well. After restimulation of cytokine-containing panels (described below), cells were stained with
128 eBioscience Fixable Viability Dye eFluor 506 (Invitrogen) diluted 1/1,000 in phosphate buffered saline (PBS; Sigma-
129 Aldrich) and incubated for 30 minutes at 4°C. Then, cells were washed, stained with the surface antibody mix
130 (**Supplementary Table 1**) in FACS buffer (PBS supplemented with 2% FBS and 0.1% sodium azide) and incubated
131 for 25 minutes at 4°C. On-treatment PD-1 expression was measured indirectly using biotinylated anti-human IgG4.
132 Restimulation probably led to dissociation of nivolumab/pembrolizumab from PD-1, resulting in apparently
133 diminished PD-1 expression on-treatment. Therefore, in restimulated panels we stained PD-1 in on-treatment
134 samples with both anti-IgG4 and anti-PD-1 (clone EH12.2H7) as described previously [22]. After primary surface

staining and two washes, cells from on-treatment timepoints were stained with Brilliant Violet 711 conjugated streptavidin and incubated for 30 minutes at 4°C. Following two washes, cells were fixed and permeabilized using eBioscience fixation/permeabilization reagent (Invitrogen) and incubated for 30 minutes at 4°C. After two washes, cells were stained with intracellular and intranuclear antibody mix (**Supplementary Table 1**), incubated for 30 minutes at 4°C, washed again and finally stored in FACS buffer at 4°C. Cells were measured the same or the next day on an LSR Fortessa. Longitudinal samples from the same patient were processed in one batch, healthy donors were included in each batch and patient samples were randomized over batches with respect to ICI regimen and toxicity status. Prior to every measurement, Sphero™ Rainbow Calibration beads (BD Biosciences, San Jose, CA) were measured to confirm stable cytometer settings (**Supplementary Fig. 1A**). FlowJo software was used to analyze data; gating strategies are in **Supplementary Fig. 6A-B**.

PBMC stimulation

For flow cytometry panels that included cytokine staining, cells were stimulated prior to staining with 20 ng/ml phorbol 12-myristate 13-actetate (PMA; Sigma-Aldrich) and 1.0 µg/ml ionomycin (Sigma-Aldrich). Golgistop (containing 0.26% monensin; BD Biosciences) 1/1,500 was added 30 minutes after PMA/ionomycin. Cells were then incubated (37°C, 5% CO_2) in the presence of PMA/ionomycin and Golgistop for another 3.5 hours.

Multiplex immunoassay

Concentrations of 23 soluble factors (**Supplementary Table 2**) were measured in serum collected at the same timepoints as PBMCs by an in-house developed and validated immunoassay based on Luminex technology (xMAP, Luminex Austin, TX) at the Multiplex Core Facility (University Medical Center Utrecht) as described previously [23, 24]. Aspecific heterophilic immunoglobulins were preabsorbed with heteroblock (Omega Biologicals, Bozeman, MT) and acquisition was performed with the Biorad FlexMAP3D (Biorad laboratories, Hercules, USA) in combination with xPONENT software (v4.2, Luminex). Data was analyzed by 5-parametric curve fitting using Bio-Plex Manager software (v6.1.1, Biorad). Serum samples from 10 healthy donors other than PBMC healthy donors were obtained from the University Medical Center Utrecht Mini Donor Service (median age 35 years, range 26-61; 60% male sex). For one patient no serum was available. Values below the limit-of-detection (LOD) were replaced with 0.5×LOD. Original (extrapolated) values were kept for traceable analytes below LOD but above 0.5×LOD. No values were out-of-range above maximal detectable levels.

Unsupervised analysis

All statistical analyses were performed with R version 4.2.0. For principal component analysis (PCA), missing data were imputed with the population median per parameter and PCA was performed using *prcomp()* in *stats* (v3.6.2) on all 159 read-out parameters across all panels (**Supplementary Table 1**). t-Distributed stochastic neighbor

169 embedding (t-SNE) projections for the T cell cytotoxicity panel (panel 2, **Supplementary Table 1**) were created
170 using *Rtsne* (θ=0.5; v0.16) for pre-gated alive $CD3^+$ singlets in a concatenated file containing a subset of 10% of all
171 cells randomly drawn from samples upon timepoint 3, toxicity or healthy donor. All cluster of differentiation proteins
172 except CD3 were used as input parameters for t-SNE. Self-organizing map (SOM) visualizations were created on
173 the same concatenated file (with 100% of the cells and the same parameters as used for t-SNE) using *FlowSOM*
174 (v2.4.0) [ref. 25], clustered by k-means clustering, and finally overlaid with manual gating results to confirm gating
175 strategy accuracy.
176
177 **Statistical analysis**
178 Longitudinal continuous data were analyzed by linear mixed effects models using the *nlme* package (v3.1-158).
179 Random intercept for subject models with fixed effects for ICI regimen, toxicity status and their interaction with time
180 were fit by restricted maximum likelihood. Significance for fixed effects was evaluated with Satterthwaite
181 approximations, to achieve conservative estimates in mixed effects models with relatively small sample size [26].
182 Model output was visualized as predicted population estimates with 95% confidence intervals (CIs). Mean and 95%
183 CI (by one-sample t-test) for healthy donor values was plotted as solid and dashed grey lines, respectively.
184 Continuous variables were analyzed with one-sample t tests for single groups, or a Wilcoxon rank sum test (for
185 unpaired) or Wilcoxon signed-rank test (for paired data) between two groups. More than two groups were compared
186 with the Kruskal-Wallis test followed by Dunn's post-hoc test with Benjamini-Hochberg false discovery rate
187 correction. P values <0.05 (two-sided) were considered statistically significant.
188
189 **Ethical approval**
190 The UNICIT biobank study was not considered subject to the Dutch Medical Research with Human Subjects Law
191 by the medical research ethics committee of the University Medical Center Utrecht. The biobank review committee
192 of the University Medical Center Utrecht approved the UNICIT biobank protocol (TCbio 18-123) and granted
193 permission for use of human biospecimens for the present study (TCbio 19-704). All participants provided written
194 informed consent in line with the Declaration of Helsinki.
195
196 **Results**
197 **Patient characteristics**
198 Longitudinal blood samples collected at baseline, at ±3 weeks (Timepoint 2) and at ±6 weeks or upon irAEs before
199 immunosuppression (Timepoint 3/Toxicity) from 44 ICI-treated patients (12 anti-PD-1 monotherapy with clinically
200 relevant irAEs [TOX], 12 anti-PD-1 monotherapy without clinically relevant irAEs [NOTx], 10 combined ICI [cICI]
201 TOX and 10 without TOX [cICI NOTx]) were included, along with 10 healthy donors (HD) (**Fig. 1**, **Table 1**,
202 **Supplementary Table 3**). As expected for cICI TOX, these patients had more concomitant, earlier-onset and more

203 **Table 1. Characteristics of patients and healthy donors**

	Anti-PD-1 NOTx (N=12)	Anti-PD-1 TOX (N=12)	cICI NOTx (N=10)	cICI TOX (N=10)	Healthy donor (N=10)	*P* value
Age (yr)						
Median (IQR)	63.5 (58.5-69.25)	72.5 (65.5-76.25)	71.0 (58.25-75)	49.5 (45.5-62.75)	56.0 (38.75-60.75)	**<0.01**
Sex (male), N (%)	8 (66.7)	9 (75.0)	10 (100)	8 (80.0)	3 (30.0)	**0.012**
Primary tumor, N (%)						
Melanoma	9 (75.0)	10 (83.3)	3 (30.0)	8 (80.0)	N/A	**<0.01**
Non-small cell lung cancer	0 (0.0)	1 (8.3)	0 (0.0)	0 (0.0)		
Renal cell carcinoma	1 (8.3)	0 (0.0)	6 (60.0)	2 (20.0)		
Urothelial cell carcinoma	2 (16.7)	0 (0.0)	0 (0.0)	0 (0.0)		
Other	0 (0.0)	1 (8.3)*	1 (10.0)#	0 (0.0)		
Tumor stage, N (%)						
III	4 (33.3)	5 (41.7)	0 (0.0)	0 (0.0	N/A	**0.011**
IV	8 (66.7)	7 (58.3)	10 (100.0)	100 (100.0)		
Time-to-toxicity (weeks)						
Median (range)	N/A	8.5 (3-20)	N/A	5 (3-12)	N/A	0.063
Number of toxicities						
1	N/A	9 (75.0)	N/A	5 (50.0)	N/A	**0.044**
2		3 (25.0)		2 (20.0)		
3		0 (0.0)		2 (20.0)		
>3		0 (0.0)		1 (10.0)		
Highest grade (CTCAE v5)						
II	N/A	9 (75.0)	N/A	0 (0.0)	N/A	**<0.01**
III		2 (16.7)		8 (80.0)		
IV		1 (8.3)		2 (20.0)		
Preexistent autoimmune disease, N (%)	0 (0.0)	0 (0.0)	1 (10.0)	0 (0.0)	0 (0.0)	0.45

**Squamous cell carcinoma of unknown primary, #Mismatch repair deficient colorectal cancer. Groups are compared by Kruskal-Wallis (continuous variables) or Fisher's exact test (categorical variables). Abbreviations: anti-PD-1 denotes 'anti-PD-1 monotherapy', cICI 'combined immune checkpoint inhibition', CTCAE 'Common Terminology Criteria for Adverse Events', IQR 'interquartile range', N/A 'not applicable', NOTx 'no clinically relevant irAEs', TOX 'with clinically relevant irAEs', yr 'years'.*

204

205 severe irAEs than anti-PD-1 TOX patients (**Table 1**). Baseline absolute eosinophil count, monocyte-to-lymphocyte
206 and neutrophil-to-lymphocyte ratios derived from complete blood counts were equal between TOX and NOTx
207 patients, as well as T cell-to-monocyte (TMR) ratio assessed by flow cytometry. Healthy donors had higher baseline
208 TMR than patients (P = 0.012).

209

210 **$CD4_{EM}$ T cell proliferation is strongly associated with irAEs in combined ICI**

211 We extensively characterized the dynamics of peripheral T and B cell immunity during ICI treatment and towards
212 the manifestation of toxicity using multicolor flow cytometry. No batch effects were observed (**Supplementary Fig.**
213 **1**). To explore shared features among subjects, we performed principal component analysis (PCA) with all 159
214 readout parameters from the measured panels in **Supplementary Table 1** pooled together. cICI TOX patients,
215 especially on-treatment timepoints, partially separated from all other subjects, including healthy donors, mainly
216 through principal component 2 (**Fig. 2A**, **Supplementary Table 4**).

217 Based on the expression of CD27 and CD45RA, distributions of $CD4^+$ and $CD8^+$ T effector memory (EM,
218 $CD27^-CD45RA^-$), central memory (CM, $CD27^+CD45RA^-$), terminally differentiated effector memory re-expressing
219 CD45RA (EMRA, $CD27^-CD45RA^+$) and naive ($CD27^+CD45RA^+$) subsets were analyzed. Although pre-treatment
220 $CD4_{EM}$ frequency has been reported as irAE predictor [11], baseline proportions of $CD4^+$ and $CD8^+$ T subsets were

221 similar between TOX and NOTx patients (**Supplementary Fig. 2A**). Compared to ICI-treated patients, healthy
222 donors had fewer $CD4_{EM}$ T cells and more naive $CD8^+$ T cells (**Supplementary Fig. 2A**). During ICI treatment, and
223 even upon onset of irAEs, relative frequencies of naive/memory subsets remained unchanged, except for an
224 increase in $CD8_{EM}$ T cells in cICI TOX (**Supplementary Fig. 2B**). However, group-specific differences in
225 proliferation (based on Ki67) over time were present. A significant increase in $CD4_{EM}$ proliferation from baseline to
226 Timepoint 2 was observed in all cICI TOX patients, but not in cICI NOTx patients (**Fig. 2B**). To enable comparison
227 of all five groups (TOX or NOTx in anti-PD-1 monotherapy or cICI and healthy donors) simultaneously and over
228 time, we graphically summarized patient-level data by plotting group-specific linear mixed models. cICI TOX, but
229 not NOTx or anti-PD-1-treated patients showed significantly increased proliferation in $CD4_{EM}$, $CD4_{CM}$, $CD8_{EM}$,
230 $CD8_{CM}$ and $CD8_{EMRA}$ T cells (**Fig. 2C,D**, **Supplementary Fig. 2C-E**).
231 While the latter effects pertain to the (early) effects of ICI treatment, we were also interested in baseline
232 parameters associated with irAE development. Higher $CD4_{EM}$ proliferation before the first ICI administration was
233 associated with shorter time-to-toxicity (ρ = -0.53, P = 0.013), but this association was entirely driven by the cICI
234 group (ρ = -0.67, P = 0.034, **Fig. 2E**). In most cICI treated TOX patients, the increase in Ki67 expression reached
235 a plateau at 3 weeks after ICI initiation (**Fig. 2B**). Both cICI TOX patients with longest time-to-toxicity developed
236 hypophysitis, a presumably complement-mediated irAE with distinct pathogenesis from most other toxicities [27].
237 This further strengthens the association of baseline $CD4_{EM}$ proliferation with early-onset toxicity after cICI.
238
239 **Th1- and Th17-associated immune responses primarily delineate irAEs after combined ICI, while anti-PD-1**
240 **TOX features only a modest Th1-associated response**
241 Expanding further on the $CD4^+$ compartment, we investigated immune response skewing by the percentages of
242 $CXCR3^+CCR4^-$, IFN-γ^+ and IL-17^+ $CD4^+$ T cells. Relative abundance of all three subsets remained constant over
243 time and neither correlated with ICI regimen, nor with toxicity development (data not shown). Although we found no
244 differences in the percentage of IFN-γ^+ $CD4^+$ T cells over time (**Fig. 3A**), cycling $CXCR3^+CCR4^-$ (Th1-associated)
245 $CD45RO^+$ memory $CD4^+$ T cells were dominant in cICI TOX relative to all other groups (**Fig. 3B**). Correspondingly,
246 we observed increased proliferation of $CXCR3^+$ $CD45RO^+$ memory $CD8^+$ T cells in cICI TOX patients
247 (**Supplementary Fig. 3A**). These findings were corroborated by serum multiplex data, which showed increased
248 serum levels of Th1-associated cytokines IL-12, TNF-α and IFN-γ in cICI TOX, and CXCL9 and CXCL10 both in
249 anti-PD-1 and cICI TOX upon Timepoint 3/Toxicity (**Fig. 3C,D**, **Supplementary Fig. 3B,C**).
250 We further characterized the kinetics of IL-17 producing $CD4^+$ T cells, which is especially relevant since
251 inhibition of Th17 differentiation by the IL-6 receptor blocker (IL-6RB) tocilizumab is clinically being tested to
252 uncouple ICI toxicity from efficacy [28]. After the first treatment cycle, cICI TOX, but not anti-PD-1 TOX or NOTx
253 patients demonstrated a vast increase in IL-17^+ T cells (**Fig. 3E**, **Supplementary Fig. 3D**). Ki67 expression in IL-
254 17^+ $CD4^+$ T cells was non-significantly higher in TOX compared to NOTx across all timepoints, including baseline,

255 regardless ICI regimen (**Supplementary Fig. 3E**). The relative decrease of IL-17$^+$ T cells from timepoint 2 to irAE
256 onset in cICI TOX is likely due to relative expansion of other subsets, as serum concentrations of Th17-associated
257 cytokines IL-6, IL-23 and IL-17 remained stable or even increased for most cICI TOX patients from Timepoint 2
258 towards irAE onset (**Fig. 3C**, **Supplementary Fig. 3B,C**).
259 Together, our data confirm that cICI TOX is largely Th1/Th17 driven, while anti-PD-1 TOX only features
260 modest Th1 enhancement relative to anti-PD-1 NOTx as assessed by serum multiplex data. Furthermore, these
261 human data suggest that IL-6RB therapy to mitigate ICI toxicity may be more effective in cICI than in anti-PD-1
262 monotherapy, although preclinical models have demonstrated its efficacy both in anti-CTLA-4 and anti-PD-1
263 monotherapies [28].
264
265 **PD-1$^+$LAG-3$^+$ CD8$^+$ T cells bear intact inflammatory and cytotoxic potential regardless development of irAEs**
266 Next, we investigated the cytotoxic potential of CD4$^+$ and CD8$^+$ T cells in relation to co-inhibitory receptor
267 expression. We used CD95 expression to select for the antigen-experienced CD8$^+$ T cell pool [29], which largely
268 overlaps with CD45RO$^+$ memory cells but also includes T_{EMRA}s (**Fig. 4A**). First, we created t-SNE and FlowSOM
269 visualizations on a representative sample of alive CD3$^+$ singlets from Timepoint 3/Toxicity across all patients and
270 healthy donors to explore the variety of subsets in an unbiased way. Proinflammatory cells with high potential for
271 IFN-γ production were represented mainly across the CD8$^+$ compartment (**Fig. 4B**). Within the CD8$^+$ compartment,
272 granzyme B production was especially high in the subset expressing senescence marker CD57 (**Fig. 4B**). Although
273 this subset appeared brighter in the anti-PD-1 and cICI TOX density plots (**Fig. 4B**), we found no statistical
274 difference in CD57$^+$ CD8$^+$ T cell abundance between groups at Timepoint 3/Toxicity. Labels assigned based on
275 manual gating matched unsupervised clustering results, demonstrating that our gating strategy adequately covers
276 relevant biological variation (**Supplementary Fig. 4A**).
277 Subsequentially, we investigated co-expression patterns of classical exhaustion markers PD-1 and LAG-3. At
278 baseline, PD-1$^+$LAG-3$^+$ double-positive (DP) CD8$^+$ T cells were least prevalent across groups, while DP CD4$^+$ T
279 cells were higher and made up the largest fraction of CD4$^+$ T cells in both TOX and NOTx patients, compared to
280 healthy donors (**Fig. 4C**). We found no differences in expression patterns of PD-1 and LAG-3 occurring between
281 TOX and NOTx post-treatment (**Supplementary Fig. 4B**).
282 Since merely expression of inhibitory receptors is not indicative of differentiation or functional status, we
283 assessed proinflammatory and cytotoxic capacity by measurement of IFN-γ and granzyme B production after
284 restimulation with PMA and ionomycin. Compared to double-negative (DN) T cells, a much larger proportion of DP
285 (and to a lesser extent PD-1$^+$LAG-3$^-$) CD8$^+$ T cells produced IFN-γ (**Fig. 4D**,**E**). This indicates preserved
286 proinflammatory potential of DP cells and is supported by transcriptomic data in circulating PD-1$^+$TIGIT$^+$ CD8$^+$ T
287 cells, mostly co-expressing LAG-3, in melanoma and Merkel cell carcinoma [30]. In contrast, we found that
288 granzyme B production was drastically lower in DP relative to DN CD8$^+$ T cells, regardless timepoint or the

289 development of irAEs (**Supplementary Fig. 4C,D**). Still, cICI TOX featured a profound increase in $CD8^+$ granzyme
290 B production over time relative to other groups, especially in the DP subset (**Fig. 4F**, **Supplementary Fig. 4E,F**).
291 In conclusion, our data suggest remaining cytokine production potential in supposedly senescent $CD57^+$ $CD8^+$
292 T cells. Moreover, PD-1^+LAG-3^+ DP $CD8^+$ T cells retain their proinflammatory and cytotoxic potential, while towards
293 irAEs after cICI the fraction of granzyme B producing cells increases especially in this DP subset.
294
295 **No changes in B cell subsets are observed, but serum cytokine levels indicate germinal center activation**
296 **in combined ICI TOX**
297 Then we set out to analyze the $CD19^+$ B cell compartment over time. Although early increase in $CD21^{lo}$ B cells
298 (mainly representing a memory subset) has been associated with irAEs following cICI [12, 31], we found no changes
299 in $CD21^{lo}$ B cells following ICI, while $CD27^+$ memory B cells in cICI TOX even decreased (**Fig. 5A,B**). Moreover, we
300 observed no B cell activation, measured by CCR6 expression (**Supplementary Fig. 5A**). The fraction of IgM^- class-
301 switched B cells also remained unchanged over time in all groups (**Supplementary Fig. 5B**). Despite lacking
302 indications for B cell activation and maturation based on flow cytometry data, increasing serum levels of APRIL,
303 CXCL13 and IL-21 towards toxicity suggest germinal center activity or tertiary lymphoid structure (TLS) formation,
304 again especially in cICI TOX (**Fig. 5C**, **Fig. 3C**, **Supplementary Fig. 3B,C**). Besides, higher $CD27^+CD38^{hi}$
305 plasmablast abundance at baseline was associated with shorter time-to-toxicity in cICI TOX (**Fig. 5D**). In sum, these
306 data support a role for adaptive humoral immunity following cICI that is more pronounced in TOX than NOTx,
307 although no changes of B cell abundances were observed in peripheral blood.
308
309 **Regulatory activity by Tregs is preserved upon systemic inflammation in the context of irAEs**
310 Finally, we sought to characterize the response of regulatory T (Treg) cells after ICI treatment. While anti-CTLA-4
311 antibodies have been shown to preferentially deplete intra-tumoral CTLA-4^{hi} Tregs, their peripheral abundance is
312 maintained with anti-CTLA-4 treatment [32]. Abundance of forkhead box protein 3 $(FOXP3)^+$ $CD25^+$ $CD4^+$ Tregs
313 increased over time, especially in cICI TOX patients (**Fig. 6A**). Already at baseline, Tregs from patients showed
314 higher expression of T-box transcription factor TBX21 (T-bet) compared with healthy donors (**Fig. 6B**). This may
315 be indicative of a more activated Th1-polarized state, even before the introduction of ICI. To assess whether Tregs
316 can adequately respond to systemic inflammation inflicted by ICI, we compared expression levels of co-inhibitory
317 and co-stimulatory receptors. At Timepoint 3/Toxicity, mainly cICI TOX patients clustered together, marked by
318 upregulation of CTLA-4, ICOS and TIGIT (**Fig. 6C**). Notably, the only two cICI TOX patients with grade 4 irAEs
319 clustered distinctly, characterized by Tregs that failed to upregulate CTLA-4 or TIGIT. In sum, these findings indicate
320 that peripheral Treg function upon systemic inflammation is generally preserved after ICI, while Treg dysfunction
321 may contribute to more severe irAEs.
322

323 **Discussion**

324 Longitudinal studies into mechanisms underlying irAEs can importantly contribute to establishing evidence-based
325 treatment strategies. Therefore, we studied lymphocyte dynamics in peripheral blood of healthy donors and ICI-
326 treated patients, including patients that developed irAEs, from baseline to several weeks into treatment. Key findings
327 are that cycling Th1-associated effector memory $CD4^+$ T cells appear important drivers of acute irAEs, specifically
328 in cICI. Besides, Th17- and Th2-associated responses contribute to the development of irAEs following cICI, but
329 no changes in abundance or activation of B cell subsets were found. In contrast, anti-PD-1-associated irAEs were
330 characterized by a modestly enhanced Th1 response compared to anti-PD-1-treated patients without irAEs. This
331 likely relates to the less acute nature of anti-PD-1 associated toxicity. We showed that peripheral blood $PD\text{-}1^+LAG\text{-}$
332 3^+ $CD8^+$ T cells retained their proinflammatory potential and that especially within this DP subset the fraction of
333 granzyme B producing cells increases towards cICI TOX relative to other patient groups.

334 ICI may reinvigorate antitumor responses in different non-terminally exhausted cell populations. PD-
335 $1^+LAG\text{-}3^+$ (DP) T cells constitute one of these subsets. We showed that these cells produced highest amounts of
336 IFN-γ after restimulation with PMA and ionomycin, which may indicate intact proinflammatory potential *in vivo*.
337 Several aspects need to be considered to this end. First, the compartment at study (i.e., peripheral blood, lymphoid
338 or peripheral tissue) is crucial, as phenotypically similar T cells exert differential function when comparing tumor-
339 free tissue T cells to tumor-infiltrating lymphocytes [33]. Second, pan-cancer cytotoxic T cell transcriptomic studies
340 indeed show overlap of proinflammatory genes and exhaustion markers [34, 35], but *ifng* translation may be
341 hampered through posttranscriptional processes in dysfunctional T cells [36]. In addition to IFN-γ production, cICI
342 TOX featured a profound increase in granzyme B production over time, especially in DP $CD8^+$ T cells. This relative
343 expansion may be due to reinvigoration of dysfunctional cells, which already express co-inhibitory receptors.
344 Alternatively, cells may be activated *de novo*, leading to co-inhibitory receptor upregulation portraying the acute
345 phase of activation. In sum, our study presents DP T cells as most potent proinflammatory and cytotoxic cells, but
346 to what extent this potential is deployed *in vivo* is likely dependent on ICI regimen and warrants further investigation.

347 $CD57^+$ terminally differentiated effector $CD8^+$ T cells form another subset that has been implicated in the
348 response to ICI. We found that $CD57^+$ $CD8^+$ T cells were non-significantly higher in ICI-treated patients (especially
349 in those with toxicity) compared to healthy donors, probably indicating cancer-induced T cell senescence. However,
350 percentages $CD57^+$ $CD8^+$ T cells remained unchanged over time. This is line with a study by Fehlings et al. who
351 reported that $CD57^+$ fractions were similarly abundant before and after ICI treatment [37]. The latter study showed
352 that a circulating $CD57^+$ cluster with enhanced cytotoxicity exhibited increased clonality and more often shared TCR
353 clonotypes with tumor tissue after ICI than other $CD8^+$ populations [37]. Since $CD57^+(CD8^+)$ cells may be sustained
354 by self-renewal capacity independent of TCR engagement or co-stimulation [38], this population possibly contributes
355 to irAE development independent of CD4 help.

356 PD-1$^+$CD8$^+$ T cells are the primary cells proliferating in response to ICI [39, 40], and proliferative response
357 is further enhanced with co-expression of multiple inhibitory receptors [40]. In cICI TOX we observed ongoing
358 proliferation in the CD8$^+$ and, most prominently, CD4$^+$ memory pools. Actually, our study may have underestimated
359 the effect of ICI on peripheral T cell proliferation. Cycling CD8$^+$ T cells have namely been shown to peak at seven
360 days after anti-PD-1 treatment before they gradually return towards baseline levels three weeks post-treatment
361 [41], possibly because of migration of proliferating cells into tissues. Our results are in line with other studies
362 indicating increased CD4$^+$ and CD8$^+$ clonal expansion and repertoire diversification in patients with irAEs [11, 16,
363 42-44]. Moreover, CD4$_{EM}$ T cell expansion in patients with irAEs parallels CD4 memory abundance in classical
364 autoimmune disease [11]. Together, these data reinforce the hypothesis that cross- or autoreactive CD4$_{EM}$ clones
365 may be unleashed upon ICI treatment in some, especially early, irAEs.

366 Helper T cells may also provide help to autoantibody-producing B cells. In line with an antibody-mediated
367 etiology, our serum cytokine data (including CXCL13 and IL-21) suggest germinal center activation or TLS formation
368 both in cICI and anti-PD-1 monotherapy irAEs. CD4$_{EM}$ T cells have been shown to contribute to thyroiditis
369 development in anti-PD-1 treated mice with preexisting autoimmunity following anti-thyroglobulin immunization [14].
370 This underscores that autoantibodies are likely at stake in some irAEs, including those affecting the thyroid gland
371 [45]. Recent work by Johannet et al. showed that baseline serum autoantibody signatures are predictive of severe
372 irAEs (not limited to thyroiditis) with adjuvant anti-PD-1 and/or anti-CTLA-4 [46], which presents further evidence
373 that preexistent subclinical autoimmunity may be at the root of various irAEs. Importantly, CXCL13 increase does
374 not *per se* indicate TLS formation, as tumor-reactive T cells identified through *CXCL13* expression can also be a
375 source that expands upon treatment in ICI-responders [47].

376 The role of B cells in irAE development is further solidified by human data on increasing CD21^{lo} B cells in
377 association with irAEs in the setting of cICI [12, 31]. We were not able to reproduce these findings, but this may be
378 due to different timing in blood collection and B cells migrating quickly into peripheral tissues following activation. A
379 recent study found that aged anti-PD-1-treated mice developed TLS-like aggregates in irAE-affected tissue in a
380 CXCL13-dependent fashion and that B cell depletion could attenuate ICI-inflicted toxicity [48]. So far, the use of
381 rituximab for irAE management is limited to case reports [49]. These data together with our work reinforce B cells
382 as a potential target for irAE treatment. However, caution is warranted with such strategy as TLS activation has
383 also been strongly associated with clinical response to ICI [50].

384 Strengths of our study include the longitudinal design with multiple on-treatment timepoints, the stratified
385 analysis for anti-PD-1 and combined ICI treated patients and the variety of T and B cell related parameters that
386 were measured. This allowed investigation of very early treatment-specific immunological effects that precede irAE
387 onset. Therefore, our study importantly contributes to causal understanding of irAE mechanisms. Main limitations
388 are the uneven distribution of age and sex over groups, heterogeneity in type of irAEs and the restriction to the
389 peripheral blood compartment.

390 In conclusion, we show that the peripheral blood immune response substantially differs between patients
391 treated with cICI and anti-PD-1 monotherapy, and between cICI-treated patients with and without irAEs. Toxicity is
392 clearly dominated by enhanced Th1-associated immunity, but we showed that the Th17 pathway and possibly
393 antibody-mediated immunity also contribute to cICI toxicity. In this way, our study provides rationale to guide irAE
394 treatment schemes based on ICI regimen and to deploy specific T-cell-directed (second-line) strategies, such as
395 anti-IL-6R, especially in cICI-associated irAEs.
396
397 **Ethics approval and consent to participate**: This study was approved by the University Medical Center Utrecht
398 biobank committee (TCbio 18-123). All participants provided written informed consent in line with the Declaration
399 of Helsinki.
400 **Competing interests**: KPMS has advisory relationships with Bristol Myers Squibb, Novartis, MSD, Pierre Fabre,
401 AbbVie, received honoraria from Novartis, MSD and Roche and received research funding from BMS, Philips and
402 TigaTx. FW has advisory relationships with Janssen and Takeda, and received research funding from Takeda,
403 Galapagos, BMS, Sanofi, and Leo Pharma.
404 **Availability of data and material**: Data and scripts for statistical analysis are available upon reasonable request.
405 **Funding**: This investigator-initiated study received funding from Bristol-Myers Squibb.
406 **Authors' contributions**: Conception: FW, KPMS, MJME. Patient accrual and biobanking: RJV, MJME, ASRL,
407 KPMS. Experiments: MJME, SAW. Original draft preparation: MJME. Writing and reviewing: all authors.
408 **Acknowledgements**: We thank the patients, their families and caregivers, healthy donors, clinical staff and UNICIT
409 consortium members. We would like to thank the Multiplex Core Facility of the University Medical Center Utrecht
410 for performing the multiplex immunoassays.
411 **Collaborators UNICIT consortium**: Linde Meyaard, Jürgen H.E. Kuball, Bas Oldenburg, Jeanette H.W. Leusen.
412
413 **Figure captions**
414 **Figure 1. Design of multicolor longitudinal flow cytometry study**. Peripheral blood mononuclear cell (PBMC)
415 and serum samples from immune checkpoint inhibitor (ICI)-treated patients developing or remaining free of clinically
416 relevant immune-related adverse events (irAEs) were included at baseline, ±3 weeks into treatment and at ±6
417 weeks or upon irAE onset. Healthy donor PBMCs and serum were included for comparison. Created with
418 BioRender.com.
419
420 **Figure 2. Effector memory CD4$^+$ T cell proliferation increases over time in combined-ICI treated patients**
421 **with toxicity, relative to other groups, and is at baseline associated with early irAE onset.** (**A**) Plot showing
422 clustering of different groups in principal component analysis (PCA) with pooled flow cytometric data including all
423 159 readout parameters across panels. (**B**) Individual patient trajectories of the percentage Ki67$^+$ of CD4$^+$ effector

memory ($CD4_{EM}$) T cells. Comparison by unpaired Wilcoxon test because of missing paired data for some patients. (**C**,**D**) Percentage proliferating of total $CD4_{EM}$ (**C**) and $CD8_{EM}$ (**D**) T cells over time. Only significant coefficients from mixed-effects models for the interaction term with time ('B'), indicating statistically significant change compared to other groups, are shown. Gray solid and dashed lines indicate mean healthy donor level with 95% confidence interval. (**E**) Correlation between baseline CD_{EM} proliferation rate and time-to-toxicity, stratified by ICI-regimen (by Spearman correlation). irAE: immune-related adverse event, NS: not significant, w/o: without, * P<0.05

Figure 3. Both Th1- and Th17-associated immune responses are observed in combined-ICI treated patients with toxicity, whereas only enhanced Th1-associated immunity is associated with anti-PD-1 associated toxicity. (**A**,**B**) Percentage IFN-γ^+ of total $CD4^+$ T cells (**A**) and percentage proliferating of $CXCR3^+CCR4^-$ Th1-associated $CD4^+$ T cells (**B**) over time. Only significant coefficients from mixed-effects models for the interaction term with time ('B'), indicating statistically significant change compared to other groups, are shown. Gray solid and dashed lines indicate mean healthy donor level with 95% confidence interval. (**C**) Heatmap showing serum levels of cytokines and chemokines after ±6 weeks (T3), upon irAE onset (Toxicity) or in healthy donors. Data are scaled by individual proteins across timepoints (see **Supplementary Fig. 3B**,**C**), enabling direct comparison of individual proteins between three timepoints. Unsupervised clustering of patients by Manhattan distance. (**D**) Volcano plot showing relative increase in serum protein levels at Timepoint 3/Toxicity in all patients with irAEs (TOX; anti-PD-1 and cICI combined) versus all patients without irAEs (NOTx). Full protein names are in **Supplementary Table 2**. (**E**) Fold-change in percentage IL-17^+ of $CD4^+$ T cells relative to baseline in cICI-treated patients without irAEs (left; NOTx) and with (right; TOX) irAEs. irAE: immune-related adverse event, NS: not significant, w/o: without.

Figure 4. PD-1^+LAG-3^+ double positive $CD8^+$ memory T cells retain their inflammatory potential regardless the development of toxicity. (**A**) Representative flow cytometry plot of CD95 and CD45RO expression in $CD8^+$ T cells. (**B**) t-SNE visualizations for a random 10% subset of all $CD3^+$ T cells from all patients at Timepoint 3/Toxicity and healthy donors, with relative abundance shown in density plots (top) and expression of lineage markers, IFN-γ and granzyme B in overlay plots (bottom). (**C**) Baseline percentages of $CD45RO^+$ $CD4^+$ (left) and $CD95^+$ $CD8^+$ (right) T cells positive for PD-1 alone or PD-1 and LAG-3. Comparisons by Kruskal-Wallis tests. (**D**,**E**) Percentages of $CD95^+CD8^+$ T cells producing IFN-γ after PMA/ionomycin stimulation, depending on inhibitory receptor expression pattern, in patients without (**D**) or with irAEs (**E**) stratified by time of sample collection; anti-PD-1- and cICI-treated patients are combined. Comparisons by pairwise paired Wilcoxon tests with Benjamini-Hochberg correction for multiple testing. (**F**) Percentage of granzyme B producing PD-1^+LAG-3^+ $CD95^+CD8^+$ T cells over time. Significant coefficient (interaction term with time; 'B') from mixed-effects model is shown. Gray solid and dashed lines indicate mean healthy donor level with 95% confidence interval. cICI: combined ICI, irAE: immune-related adverse event, NS: not significant, w/o: without. * P<0.05, ** P<0.01, *** P<0.001, **** P<0.0001.

458

459 **Figure 5. Increasing serum CXCL13 levels and higher baseline plasmablast abundance in patients with**
460 **early toxicity suggest a role for antibody-mediated immunity in toxicity after combined ICI.** (**A**-**C**)
461 Percentages of $CD21^{lo}$ (**A**) and $CD27^{+}$ memory (**B**) B cells of total B cells and serum level (in pg/ml) of CXCL13 (**C**)
462 over time. Only significant coefficients (interaction terms with time; 'B') from mixed-effects models are shown. Gray
463 solid and dashed lines indicate mean healthy donor level with 95% confidence interval. (**D**) Correlation between
464 baseline percentage $CD27^{+}CD38^{hi}$ plasmablasts of total B cells and time-to-toxicity, stratified by ICI-regimen (by
465 Spearman correlation). irAE: immune-related adverse event, w/o: without.

466

467 **Figure 6. Peripheral regulatory T cell abundance and function are generally preserved upon toxicity.** (**A**)
468 Percentage of $CD25^{+}FOXP3^{+}$ $CD4^{+}$ Treg cells of total $CD4^{+}$ T cells over time. Significant coefficient (interaction term
469 with time; 'B') from mixed-effects model is shown. Gray solid and dashed lines indicate mean healthy donor level
470 with 95% confidence interval. (**B**) Comparison of median fluorescence intensity (MFI) of T-bet in Tregs at baseline
471 between healthy donors and all ICI-treated patients, by Wilcoxon test. (**C**) Expression levels (by MFI) of inhibitory
472 and costimulatory receptors in Tregs (for patients Timepoint 3/Toxicity), hierarchically clustered by Euclidean
473 distance. irAE: immune-related adverse event, w/o: without.

474

475 **References**

476 1. Sullivan RJ, Weber JS. Immune-related toxicities of checkpoint inhibitors: mechanisms and mitigation
477 strategies. Nat Rev Drug Discov 2022;21(7):495-508. doi:10.1038/s41573-021-00259-5
478 2. Haanen JBAG, Carbonnel F, Robert C, et al. Management of toxicities from immunotherapy: ESMO Clinical
479 Practice Guidelines for diagnosis, treatment and follow-up. Ann Oncol 2018;29:iv264-iv266.
480 doi:10.1093/annonc/mdy162.
481 3. Schneider BJ, Naidoo J, Santomasso BD, et al. Management of Immune-Related Adverse Events in Patients
482 Treated With Immune Checkpoint Inhibitor Therapy: ASCO Guideline Update. J Clin Oncol 2021;39(36):4073-
483 4126. doi:10.1200/JCO.21.01440
484 4. Brahmer JR, Abu-Sbeih H, Ascierto PA, et al. Society for Immunotherapy of Cancer (SITC) clinical practice
485 guideline on immune checkpoint inhibitor-related adverse events. J Immunother Cancer 2021;9(6):e002435.
486 doi:10.1136/jitc-2021-002435
487 5. Zou F, Faleck D, Thomas A, et al. Efficacy and safety of vedolizumab and infliximab treatment for immune-
488 mediated diarrhea and colitis in patients with cancer: a two-center observational study. J Immunother Cancer
489 2021;9(11):e003277. doi:10.1136/jitc-2021-003277

490 6. Verheijden RJ, May AM, Blank CU, et al. Association of Anti-TNF with Decreased Survival in Steroid Refractory
491 Ipilimumab and Anti-PD1-Treated Patients in the Dutch Melanoma Treatment Registry. Clin Cancer Res
492 2020;26(9):2268-2274. doi:10.1158/1078-0432.CCR-19-3322
493 7. van Not OJ, Verheijden RJ, van den Eertwegh AJM, et al. Association of Immune-Related Adverse Event
494 Management With Survival in Patients With Advanced Melanoma. JAMA Oncol 2022;8(12):1794-1801.
495 doi:10.1001/jamaoncol.2022.5041
496 8. Hommes JW, Verheijden RJ, Suijkerbuijk KPM, Hamann D. Biomarkers of Checkpoint Inhibitor Induced
497 Immune-Related Adverse Events—A Comprehensive Review. Front Oncol 2021;10:585311.
498 doi:10.3389/fonc.2020.585311
499 9. Damuzzo V, Solito S, Pinton L, et al. Clinical implication of tumor-associated and immunological parameters in
500 melanoma patients treated with ipilimumab. Oncoimmunology 2016;5(12):e1249559.
501 doi:10.1080/2162402X.2016.1249559
502 10. Chaput N, Lepage P, Coutzac C, et al. Baseline gut microbiota predicts clinical response and colitis in metastatic
503 melanoma patients treated with ipilimumab. Ann Oncol 2017;28(6):1368-1379. doi:10.1093/annonc/mdx108
504 11. Lozano AX, Chaudhuri AA, Nene A, et al. T cell characteristics associated with toxicity to immune checkpoint
505 blockade in patients with melanoma. Nat Med 2022;28(2):353-362. doi:10.1038/s41591-021-01623-z
506 12. Das R, Bar N, Ferreira M, et al. Early B cell changes predict autoimmunity following combination immune
507 checkpoint blockade. J Clin Invest 2018;128(2):715-720. doi:10.1172/JCI96798
508 13. Kim KH, Hur JY, Cho J, et al. Immune-related adverse events are clustered into distinct subtypes by T-cell
509 profiling before and early after anti-PD-1 treatment. Oncoimmunology 2020;9(1):e1722023.
510 doi:10.1080/2162402X.2020.1722023
511 14. Yasuda Y, Iwama S, Sugiyama D, et al. $CD4^+$ T cells are essential for the development of destructive thyroiditis
512 induced by anti–PD-1 antibody in thyroglobulin-immunized mice. Sci Transl Med 2021;13(593): eabb7495.
513 doi:10.1126/scitranslmed.abb7495
514 15. Hutchinson JA, Kronenberg K, Riquelme P, et al. Virus-specific memory T cell responses unmasked by immune
515 checkpoint blockade cause hepatitis. Nat Commun 2021;12(1):1439. doi:10.1038/s41467-021-21572-y
516 16. Oh DY, Cham J, Zhang L, et al. Immune Toxicities Elicted by CTLA-4 Blockade in Cancer Patients Are
517 Associated with Early Diversification of the T-cell Repertoire. Cancer Res 2017;77(6):1322-1330.
518 doi:10.1158/0008-5472.CAN-16-2324
519 17. Berner F, Bomze D, Diem S, et al. Association of Checkpoint Inhibitor-Induced Toxic Effects with Shared Cancer
520 and Tissue Antigens in Non-Small Cell Lung Cancer. JAMA Oncol 2019;5(7):1043-1047.
521 doi:10.1001/jamaoncol.2019.0402
522 18. Johnson DB, Balko JM, Compton ML, et al. Fulminant Myocarditis with Combination Immune Checkpoint
523 Blockade. N Engl J Med 2016;375(18):1749-1755. doi:10.1056/NEJMoa1609214

524 19. Bayless NL, Bluestone JA, Bucktrout S, et al. Development of preclinical and clinical models for immune-related
525 adverse events following checkpoint immunotherapy: a perspective from SITC and AACR. J Immunother
526 Cancer 2021;9(9):e002627. doi:10.1136/jitc-2021-002627
527 20. Eisenhauer EA, Therasse P, Bogaerts J, et al. New response evaluation criteria in solid tumours: Revised
528 RECIST guideline (version 1.1). Eur J Cancer 2009;45(2):228-247. doi:10.1016/j.ejca.2008.10.026
529 21. NCI (National Cancer Institute). Common Terminology Criteria for Adverse Events (CTCAE) v5.0 [online]. 2017.
530 https://ctep.cancer.gov/protocoldevelopment/electronic_applications/ctc.htm#ctc_50.
531 22. Kamphorst AO, Pillai RN, Yang S, et al. Proliferation of PD-1+ CD8 T cells in peripheral blood after PD-1–
532 targeted therapy in lung cancer patients. Proc Natl Acad Sci U S A 2017;114(19):4993-4998.
533 doi:10.1073/pnas.1705327114
534 23. de Jager W, Prakken BJ, Bijlsma JWJ, Kuis W, Rijkers GT. Improved multiplex immunoassay performance in
535 human plasma and synovial fluid following removal of interfering heterophilic antibodies. J Immunol Methods
536 2005;300(1-2):124-135. doi:10.1016/j.jim.2005.03.009
537 24. Scholman RC, Giovannone B, Hiddingh S, et al. Effect of anticoagulants on 162 circulating immune related
538 proteins in healthy subjects. Cytokine 2018;106:114-124. doi:10.1016/j.cyto.2017.10.021
539 25. van Gassen S, Callebaut B, van Helden MJ, et al. FlowSOM: Using self-organizing maps for visualization and
540 interpretation of cytometry data. Cytometry A 2015;87(7):636-645. doi:10.1002/cyto.a.22625
541 26. Luke SG. Evaluating significance in linear mixed-effects models in R. Behav Res Methods 2017;49(4):1494-
542 1502. doi:10.3758/s13428-016-0809-y
543 27. Martins F, Sofiya L, Sykiotis GP, et al. Adverse effects of immune-checkpoint inhibitors: epidemiology,
544 management and surveillance. Nat Rev Clin Oncol 2019;16(9):563-580. doi:10.1038/s41571-019-0218-0
545 28. Hailemichael Y, Johnson DH, Abdel-Wahab N, et al. Interleukin-6 blockade abrogates immunotherapy toxicity
546 and promotes tumor immunity. Cancer Cell 2022;40(5):509-523.e6. doi:10.1016/j.ccell.2022.04.004
547 29. Galletti G, de Simone G, Mazza EMC, et al. Two subsets of stem-like CD8+ memory T cell progenitors with
548 distinct fate commitments in humans. Nat Immunol 2020;21(12):1552-1562. doi:10.1038/s41590-020-0791-5
549 30. Simon S, Voillet V, Vignard V, et al. PD-1 and TIGIT coexpression identifies a circulating CD8 T cell subset
550 predictive of response to anti-PD-1 therapy. J Immunother Cancer 2020;8(2):e001631. doi:10.1136/jitc-2020-
551 001631
552 31. Nishimura K, Konishi T, Ochi T, et al. CD21lo B Cells Could Be a Potential Predictor of Immune-Related Adverse
553 Events in Renal Cell Carcinoma. J Pers Med 2022;12(6):888. doi:10.3390/jpm12060888
554 32. Tarhini AA, Edington H, Butterfield LH, et al. Immune Monitoring of the Circulation and the Tumor
555 Microenvironment in Patients with Regionally Advanced Melanoma Receiving Neoadjuvant Ipilimumab. PLoS
556 One 2014;9(2):e87705. doi:10.1371/journal.pone.0087705

557 33. Wu X, Zhang H, Xing Q, et al. PD-1+ CD8+ T cells are exhausted in tumours and functional in draining lymph
558 nodes of colorectal cancer patients. Br J Cancer 2014;111(7):1391-1399. doi:10.1038/bjc.2014.416
559 34. Zheng L, Qin S, Si W, et al. Pan-cancer single-cell landscape of tumor-infiltrating T cells. Science
560 2021;374(6574). doi:10.1126/science.abe6474
561 35. Szabo PA, Levitin HM, Miron M, et al. Single-cell transcriptomics of human T cells reveals tissue and activation
562 signatures in health and disease. Nat Commun 2019;10(1):4706. doi:10.1038/s41467-019-12464-3
563 36. Salerno F, Guislain A, Freen-Van Heeren JJ, Nicolet BP, Young HA, Wolkers MC. Critical role of post-
564 transcriptional regulation for IFN-γ in tumor-infiltrating T cells. Oncoimmunology 2019;8(2):e1532762.
565 doi:10.1080/2162402X.2018.1532762
566 37. Fehlings M, Kim L, Guan X, et al. Single-cell analysis reveals clonally expanded tumor-associated CD57 $^{+}$ CD8
567 T cells are enriched in the periphery of patients with metastatic urothelial cancer responding to PD-L1 blockade.
568 J Immunother Cancer 2022;10(8):e004759. doi:10.1136/jitc-2022-004759
569 38. Morris SR, Chen B, Mudd JC, et al. “Inflammescent” CX3CR1+CD57+ CD8 T cells are generated and expanded
570 by IL-15. JCI Insight 2020;5(11):e132963. doi:10.1172/jci.insight.132963
571 39. Huang AC, Postow MA, Orlowski RJ, et al. T-cell invigoration to tumour burden ratio associated with anti-PD-1
572 response. Nature 2017;545(7652):60-65. doi:10.1038/nature22079
573 40. Huang AC, Orlowski RJ, Xu X, et al. A single dose of neoadjuvant PD-1 blockade predicts clinical outcomes in
574 resectable melanoma. Nat Med 2019;25(3):454-461. doi:10.1038/s41591-019-0357-y
575 41. Kim KH, Cho J, Ku BM, et al. The First-week Proliferative Response of Peripheral Blood PD-1+CD8+ T Cells
576 Predicts the Response to Anti-PD-1 Therapy in Solid Tumors. Clin Cancer Res 2019;25(7):2144-2154.
577 doi:10.1158/1078-0432.CCR-18-1449
578 42. Arakawa A, Vollmer S, Tietze J, et al. Clonality of CD4+ Blood T Cells Predicts Longer Survival With CTLA4 or
579 PD-1 Checkpoint Inhibition in Advanced Melanoma. Front Immunol 2019;10:1336.
580 doi:10.3389/fimmu.2019.01336
581 43. Robert L, Tsoi J, Wang X, et al. CTLA4 Blockade Broadens the Peripheral T-Cell Receptor Repertoire. Clin
582 Cancer Res 2014;20(9):2424-2432. doi:10.1158/1078-0432.CCR-13-2648
583 44. Subudhi SK, Aparicio A, Gao J, et al. Clonal expansion of CD8 T cells in the systemic circulation precedes
584 development of ipilimumab-induced toxicities. Proc Natl Acad Sci U S A 2016;113(42):11919-11924.
585 doi:10.1073/pnas.1611421113
586 45. Ghosh N, Chan KK, Jivanelli B, Bass AR. Autoantibodies in Patients With Immune-Related Adverse Events
587 From Checkpoint Inhibitors. J Clin Rheumatol 2022;28(2):e498-e505. doi:10.1097/RHU.0000000000001777
588 46. Johannet P, Liu W, Fenyo D, et al. Baseline Serum Autoantibody Signatures Predict Recurrence and Toxicity
589 in Melanoma Patients Receiving Adjuvant Immune Checkpoint Blockade. Clin Cancer Res 2022;28(18):4121-
590 4130. doi:10.1158/1078-0432.CCR-22-0404

591 47. Liu B, Zhang Y, Wang D, Hu X, Zhang Z. Single-cell meta-analyses reveal responses of tumor-reactive
592 CXCL13+ T cells to immune-checkpoint blockade. Nat Cancer 2022;3(9):1123-1136. doi:10.1038/s43018-022-
593 00433-7
594 48. Tsukamoto H, Komohara Y, Tomita Y, et al. Aging-associated and CD4 T-cell–dependent ectopic CXCL13
595 activation predisposes to anti–PD-1 therapy-induced adverse events. Proc Natl Acad Sci U S A. 2022;119(29).
596 doi:10.1073/pnas.2205378119
597 49. Deftereos SN, Georgonikou D. Effectiveness of rituximab in treating immune-checkpoint-inhibitor-induced
598 immune-related adverse events: results of a systematic review. Ann Oncol 2021;32(2):282-283.
599 doi:10.1016/j.annonc.2020.12.001
600 50. Fridman WH, Meylan M, Petitprez F, Sun CM, Italiano A, Sautès-Fridman C. B cells and tertiary lymphoid
601 structures as determinants of tumour immune contexture and clinical outcome. Nat Rev Clin Oncol
602 2022;19(7):441-457. doi:10.1038/s41571-022-00619-z

Figure 1

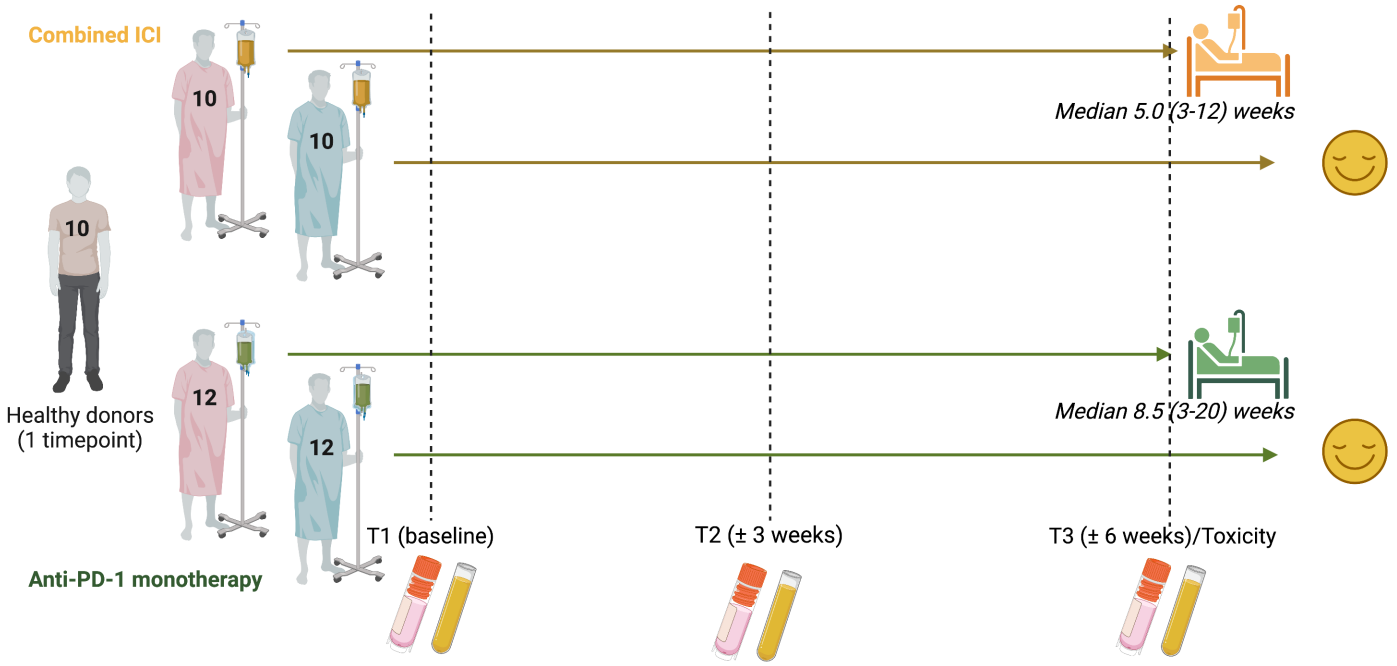
Combined ICI
10
10
10
Median 5.0 (3-12) weeks
Healthy donors
(1 timepoint)
12
12
Median 8.5 (3-20) weeks
T1 (baseline)
T2 (± 3 weeks)
T3 (± 6 weeks)/Toxicity
Anti-PD-1 monotherapy

Figure 2

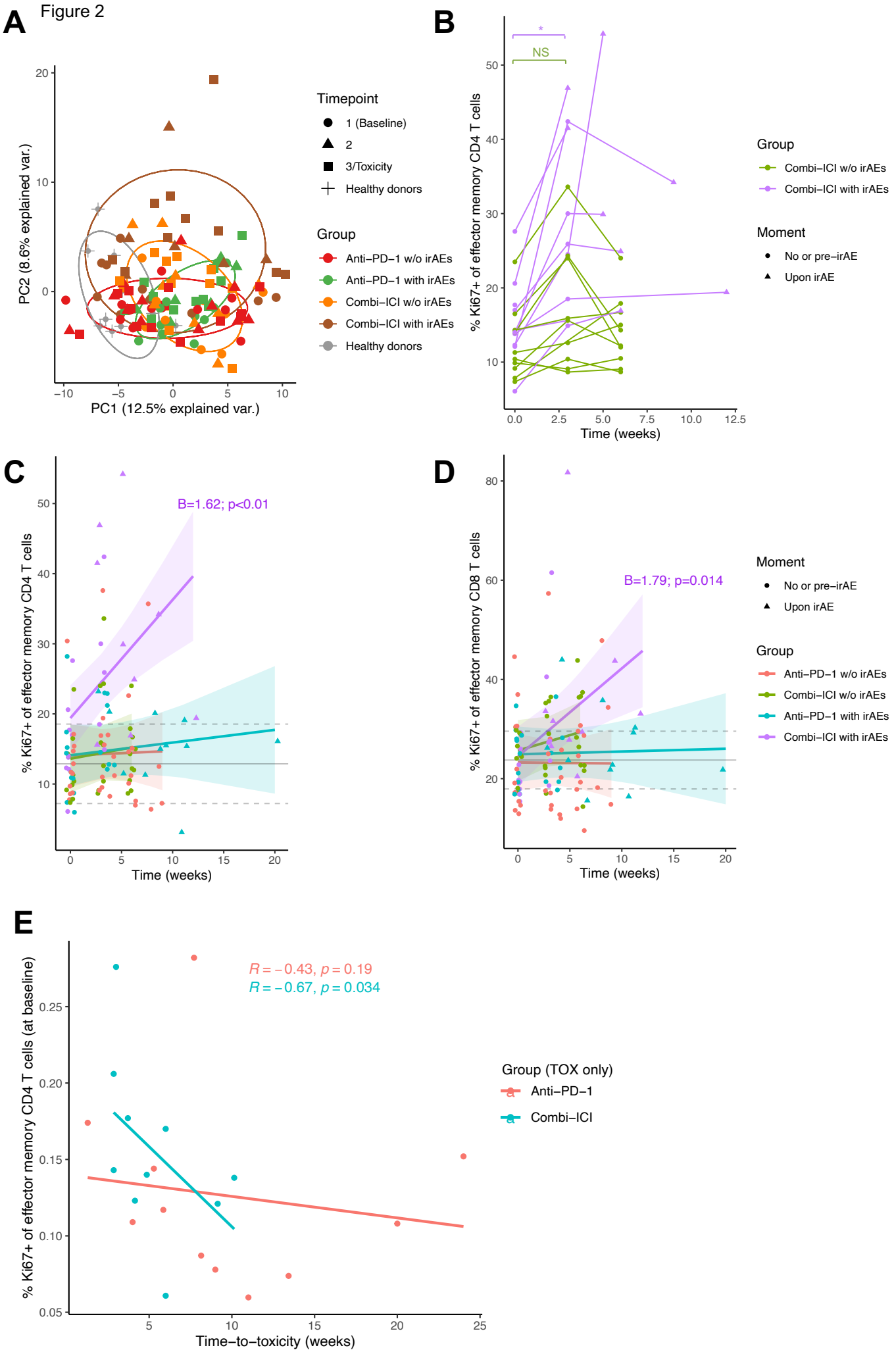
A
PC2 (8.6% explained var.)
PC1 (12.5% explained var.)
Timepoint
1 (Baseline)
2
3/Toxicity
Healthy donors
Group
Anti−PD−1 w/o irAEs
Anti−PD−1 with irAEs
Combi−ICI w/o irAEs
Combi−ICI with irAEs
Healthy donors
B
NS
% Ki67+ of effector memory CD4 T cells
Time (weeks)
Group
Combi−ICI w/o irAEs
Combi−ICI with irAEs
Moment
No or pre−irAE
Upon irAE
C
B=1.62; p<0.01
% Ki67+ of effector memory CD4 T cells
Time (weeks)
D
B=1.79; p=0.014
% Ki67+ of effector memory CD8 T cells
Time (weeks)
Moment
No or pre−irAE
Upon irAE
Group
Anti−PD−1 w/o irAEs
Combi−ICI w/o irAEs
Anti−PD−1 with irAEs
Combi−ICI with irAEs
E
R = −0.43, p = 0.19
R = −0.67, p = 0.034
% Ki67+ of effector memory CD4 T cells (at baseline)
Time−to−toxicity (weeks)
Group (TOX only)
Anti−PD−1
Combi−ICI

Figure 3

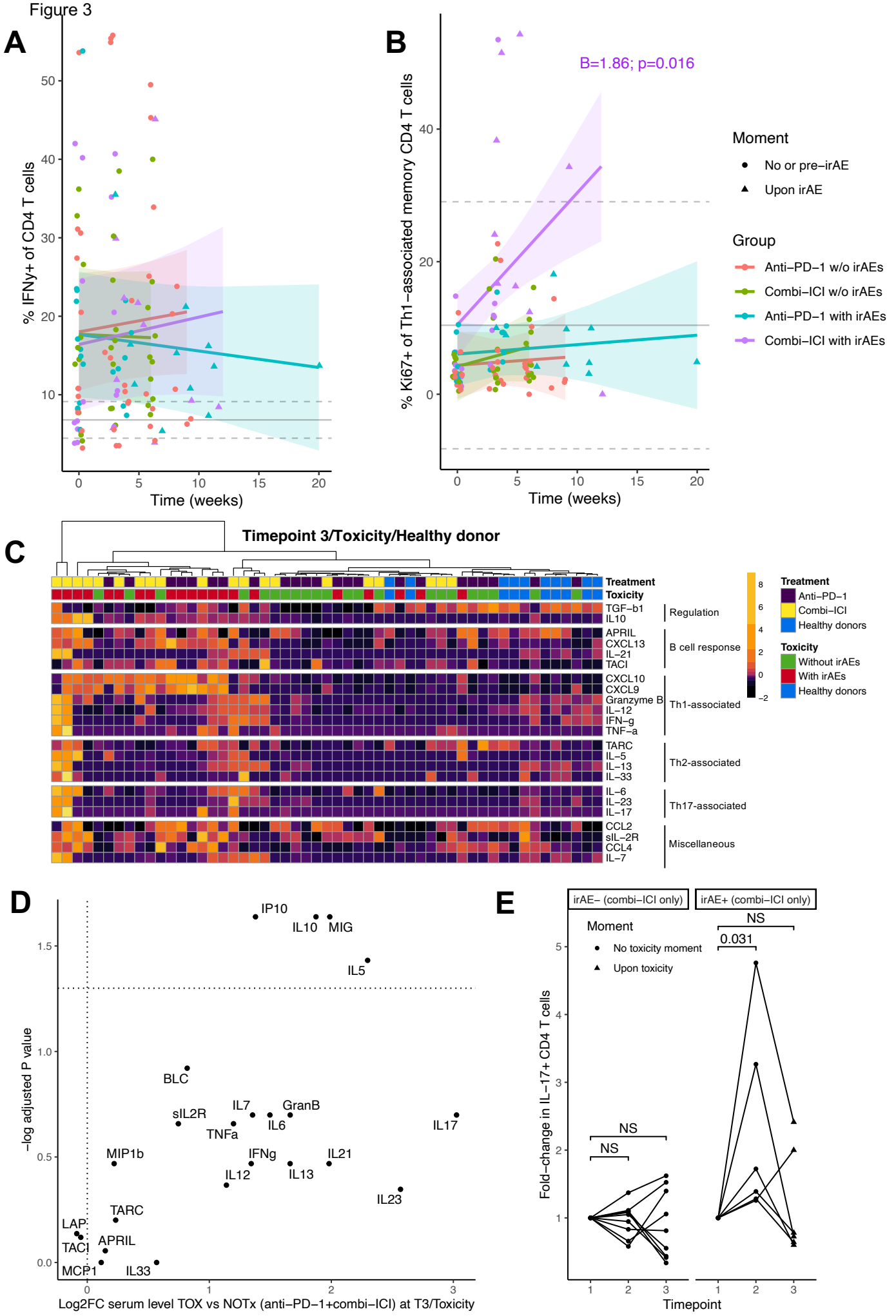
A
% IFNy+ of CD4 T cells
Time (weeks)
B
B=1.86; p=0.016
% Ki67+ of Th1−associated memory CD4 T cells
Time (weeks)
Moment
No or pre−irAE
Upon irAE
Group
Anti−PD−1 w/o irAEs
Combi−ICI w/o irAEs
Anti−PD−1 with irAEs
Combi−ICI with irAEs
C
Timepoint 3/Toxicity/Healthy donor
Treatment
Toxicity
TGF−b1
IL10
Regulation
APRIL
CXCL13
IL−21
TACI
B cell response
CXCL10
CXCL9
Granzyme B
IL−12
IFN−g
TNF−a
Th1−associated
TARC
IL−5
IL−13
IL−33
Th2−associated
IL−6
IL−23
IL−17
Th17−associated
CCL2
sIL−2R
CCL4
IL−7
Miscellaneous
Treatment
Anti−PD−1
Combi−ICI
Healthy donors
Toxicity
Without irAEs
With irAEs
Healthy donors
D
−log adjusted P value
Log2FC serum level TOX vs NOTx (anti−PD−1+combi−ICI) at T3/Toxicity
IP10
IL10
MIG
IL5
BLC
sIL2R
IL7
GranB
IL6
TNFa
IL17
MIP1b
IFNg
IL21
IL12
IL13
IL23
TARC
LAP
TACI
APRIL
MCP1
IL33
E
irAE− (combi−ICI only)
irAE+ (combi−ICI only)
Moment
No toxicity moment
Upon toxicity
NS
NS
NS
0.031
Fold−change in IL−17+ CD4 T cells
Timepoint

Figure 4

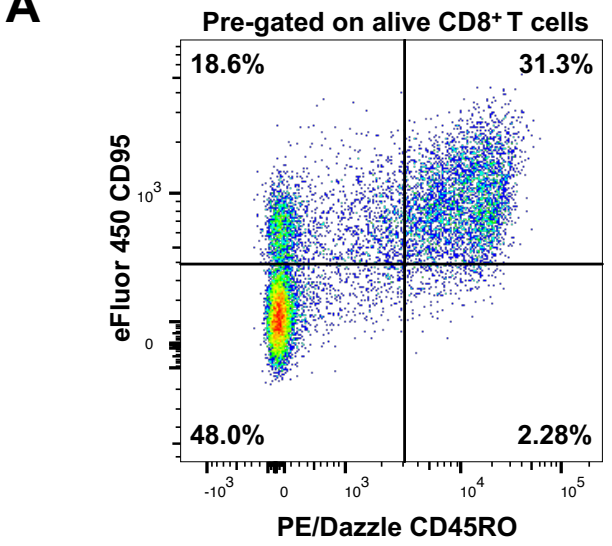
A
Pre-gated on alive CD8+ T cells
18.6%
31.3%
48.0%
2.28%
eFluor 450 CD95
PE/Dazzle CD45RO

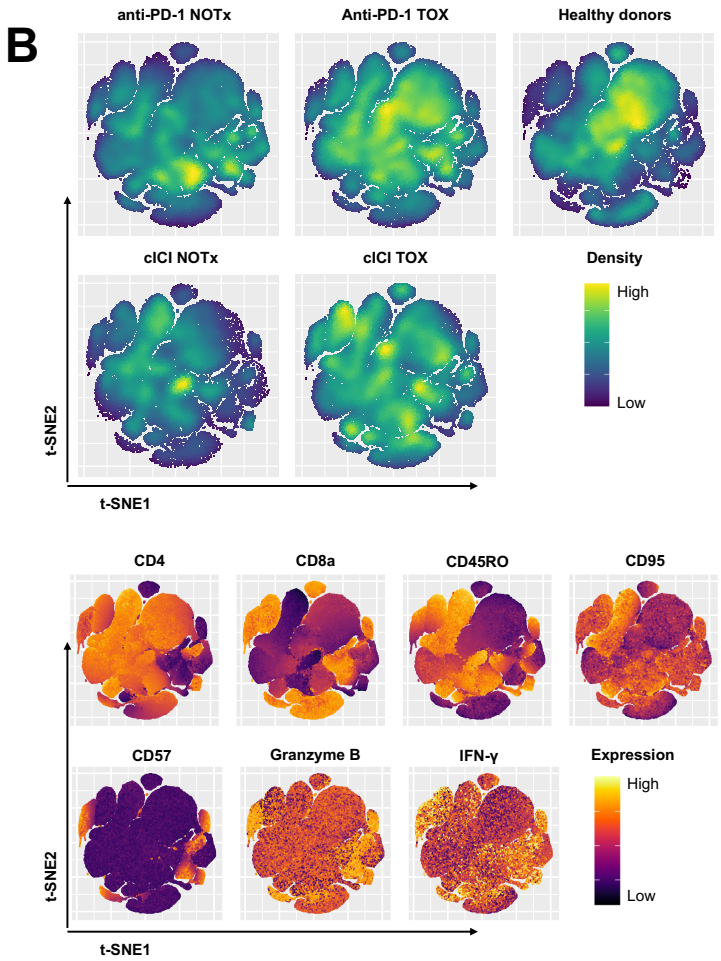
B
anti-PD-1 NOTx
Anti-PD-1 TOX
Healthy donors
cICI NOTx
cICI TOX
Density
High
Low
t-SNE2
t-SNE1
CD4
CD8a
CD45RO
CD95
CD57
Granzyme B
IFN-γ
Expression
High
Low
t-SNE2
t-SNE1

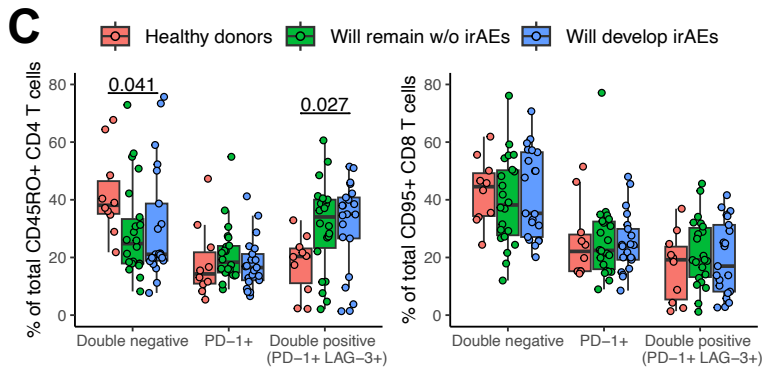
C
Healthy donors
Will remain w/o irAEs
Will develop irAEs
0.041
0.027
% of total CD45RO+ CD4 T cells
% of total CD95+ CD8 T cells
Double negative
PD−1+
Double positive (PD−1+ LAG−3+)

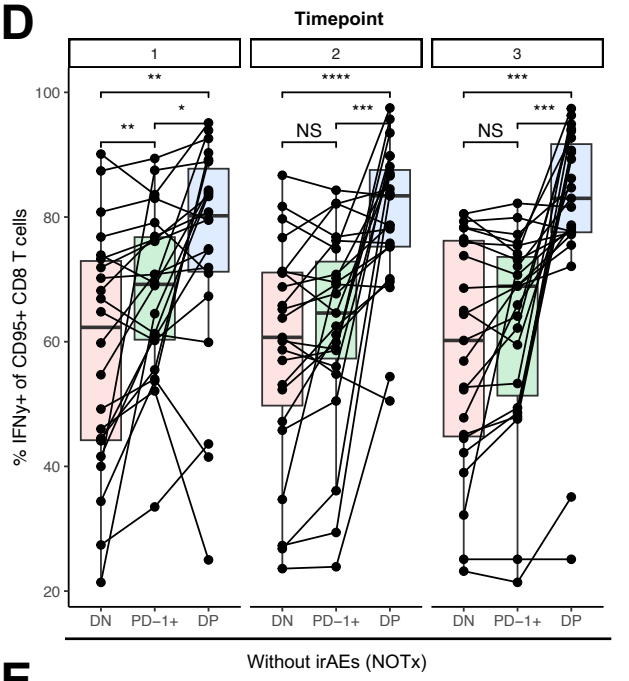
D
Timepoint
1
2
3
NS
% IFNγ+ of CD95+ CD8 T cells
DN
PD−1+
DP
Without irAEs (NOTx)

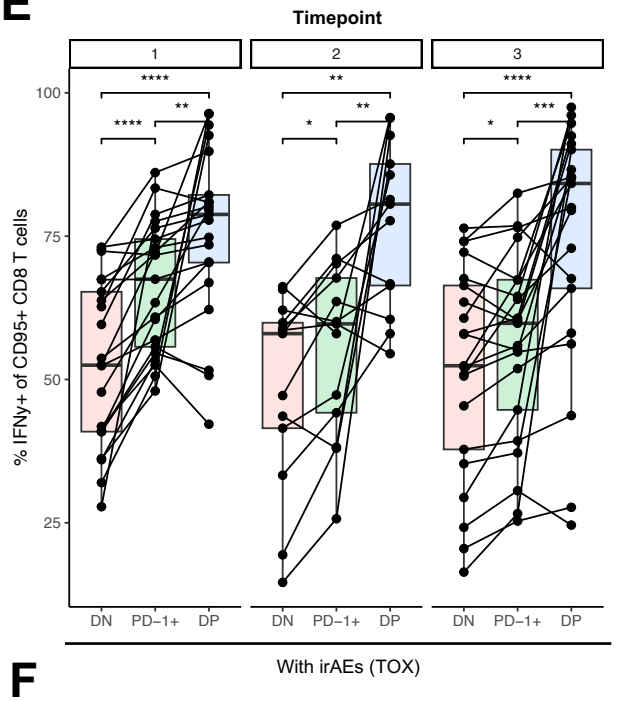
E
Timepoint
1
2
3
% IFNγ+ of CD95+ CD8 T cells
DN
PD−1+
DP
With irAEs (TOX)

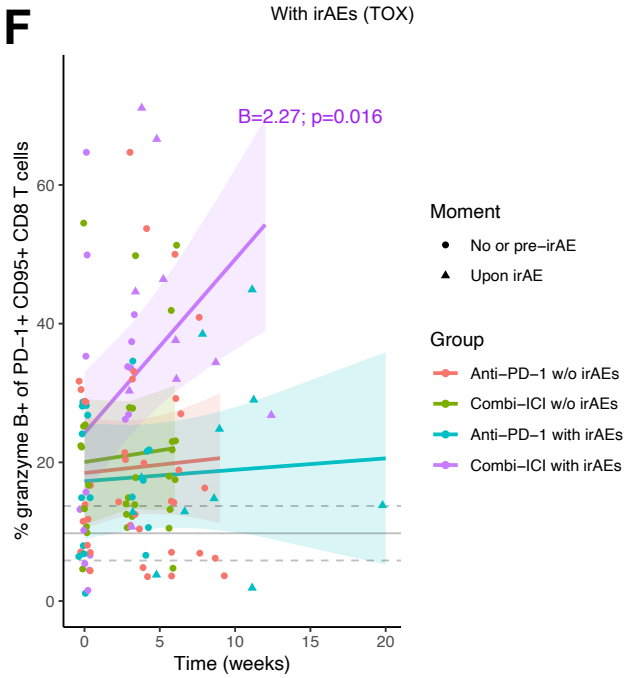
F
B=2.27; p=0.016
% granzyme B+ of PD−1+ CD95+ CD8 T cells
Time (weeks)
Moment
No or pre−irAE
Upon irAE
Group
Anti−PD−1 w/o irAEs
Combi−ICI w/o irAEs
Anti−PD−1 with irAEs
Combi−ICI with irAEs

Figure 5

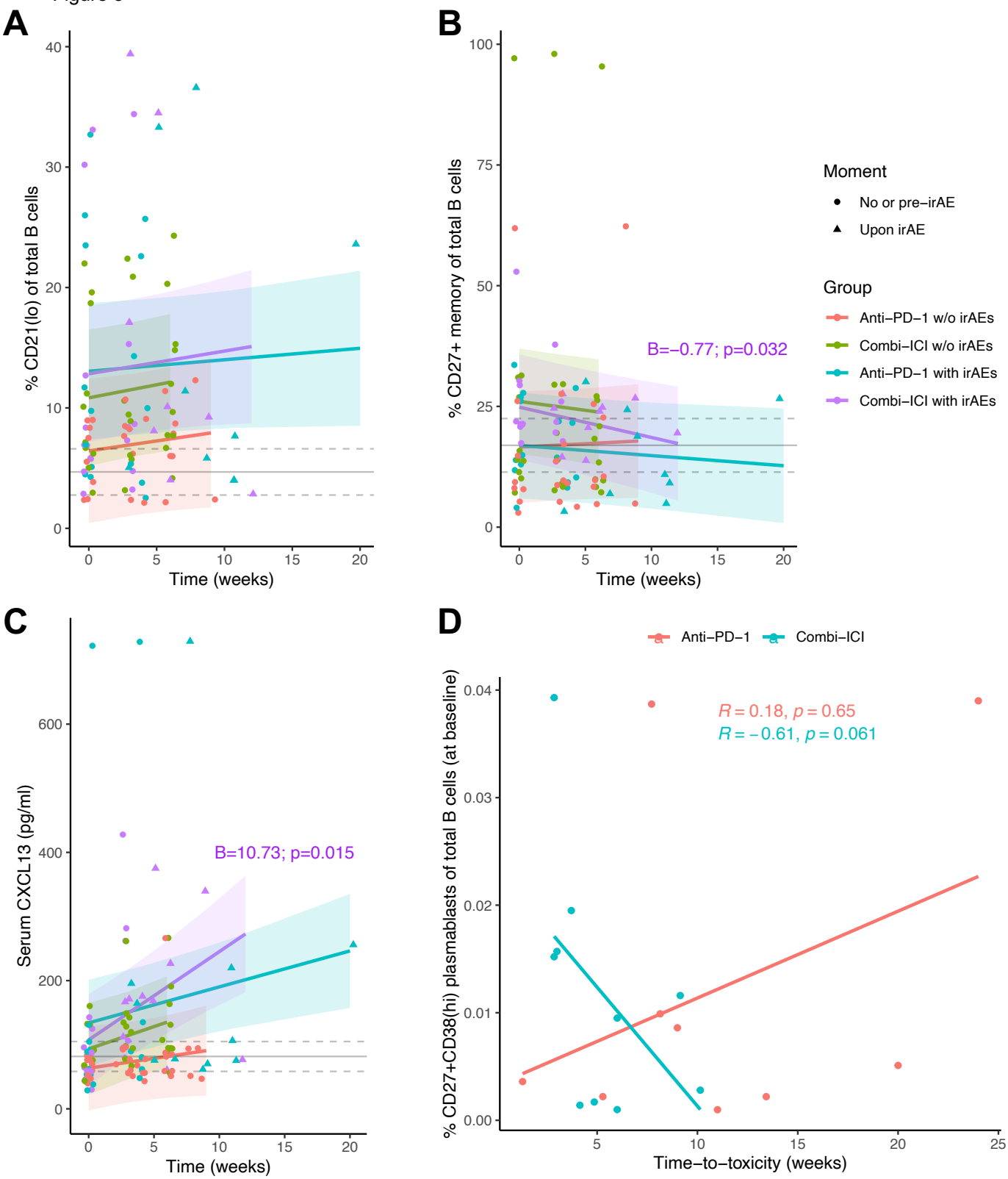
A
% CD21(lo) of total B cells
Time (weeks)
B
% CD27+ memory of total B cells
B=−0.77; p=0.032
Time (weeks)
Moment
No or pre−irAE
Upon irAE
Group
Anti−PD−1 w/o irAEs
Combi−ICI w/o irAEs
Anti−PD−1 with irAEs
Combi−ICI with irAEs
C
Serum CXCL13 (pg/ml)
B=10.73; p=0.015
Time (weeks)
D
Anti−PD−1
Combi−ICI
% CD27+CD38(hi) plasmablasts of total B cells (at baseline)
R = 0.18, p = 0.65
R = −0.61, p = 0.061
Time−to−toxicity (weeks)

Figure 6

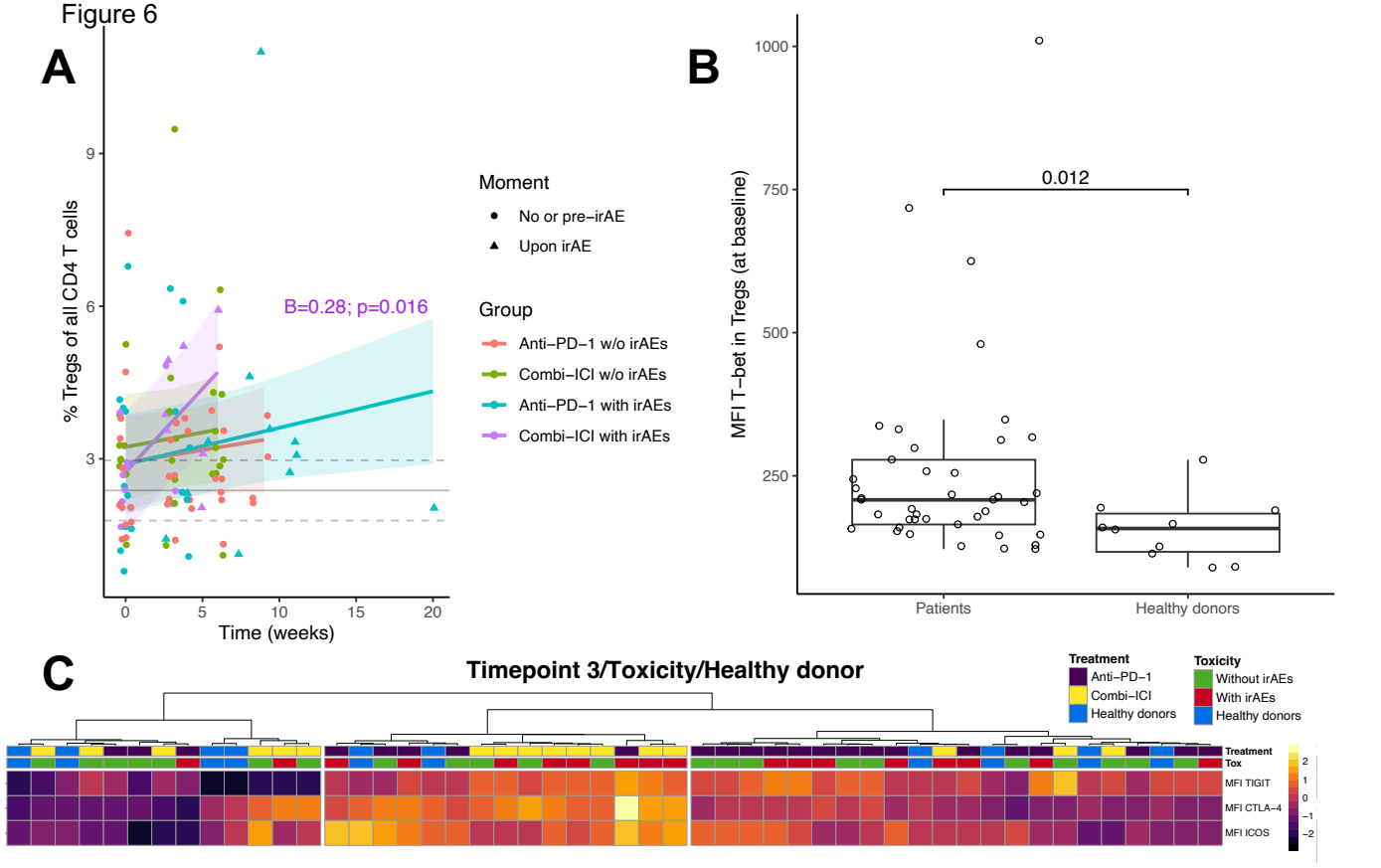
A
% Tregs of all CD4 T cells
Time (weeks)
B=0.28; p=0.016
Moment
No or pre−irAE
Upon irAE
Group
Anti−PD−1 w/o irAEs
Combi−ICI w/o irAEs
Anti−PD−1 with irAEs
Combi−ICI with irAEs
B
MFI T−bet in Tregs (at baseline)
0.012
Patients
Healthy donors
C
Timepoint 3/Toxicity/Healthy donor
Treatment
Anti−PD−1
Combi−ICI
Healthy donors
Toxicity
Without irAEs
With irAEs
Healthy donors
Treatment
Tox
MFI TIGIT
MFI CTLA−4
MFI ICOS